Pergamon

Journal of Structural Geology, Vol. 16, No. 6, pp. 883 to 893, 1994

0191-8141/94 $07.00+0.00

Initiation of folding and boudinage in wrench shear and transpression

ANDREW I. JAMES and A. JOHN WATKINSON

Department of Geology, Washington State University, Pullman, WA 99164, U.S.A.

(*Received* 7 *October* 1992; *accepted in revised form* 14 *July* 1993)

Abstract—A linear stability analysis is performed on a deforming layered three-dimensional linear viscous system. The system consists of a single layer of viscosity μ embedded in a medium of viscosity μ'. The layer is oriented normal to the z-axis and both the layer and medium are subjected to uniform simple shearing parallel to the y-axis (wrench shear) with superposed uniform shortening parallel to x and extension parallel to z (transpression). The stability of cylindrical perturbations of the form $\zeta = \mathcal{A}(t) \cos(\alpha x - \beta y)$ is examined. It is found that fold-type perturbations are unstable and pinch-and-swell disturbances are unstable in some cases. For the case of wrench shear alone the fastest growing buckling disturbances are oriented at 45° to the positive y-axis, while the fastest growing pinch-and-swell disturbances have positive growth rates and are oriented 90° to the fold axes. Additional shortening parallel to the x-axis (transpression) causes the fold axes to initiate at lower angles to the y-axis. Pinch-and-swell disturbances may or may not be unstable in transpression depending on the magnitude of stretching parallel to the z-axis.

INTRODUCTION

THEORETICAL models of fold initiation that treat rocks as slowly deforming viscous fluids have sought to illuminate the processes governing the development of instabilities in rocks. For the most part, these analyses examine two-dimensional cases of single layer folding (Biot 1957, 1959, 1961, 1964, Ramberg 1959, 1962, 1963, Treagus 1973, Smith 1975, 1977, Fletcher 1977, 1982, Alexander 1981, Wollkind & Alexander 1982) or multilayer folding (Ramberg 1970a,b, Johnson & Pfaff 1989). Naturally, these models are limited in that they were not able to examine the effects of three-dimensional strain fields or the stability of three-dimensional perturbations.

Recently, Fletcher (1991) developed a model that examined the stability of a layered viscous three-dimensional system. This model used a thick plate analysis of a layer in pure shear with the principal strain rate axes parallel and perpendicular to the plane of the layer. From this model Fletcher determined that the most unstable perturbation was a cylindrical fold-like form with its axis oriented normal to the direction of greatest shortening strain rate, except for the case where the bulk strain was pure constriction. Using Fletcher's (1991) analysis as a starting point, we consider here a model for folding of a three-dimensional layered system that examines the effect of strain fields other than pure shear. Specifically, this analysis points out the importance of the nature of the basic (or bulk) flow on the initiation of geologic structures. We seek to demonstrate that the basic flow has a great influence on the types, orientations and growth rates of geologic structures which form.

As an example we study the stability of a horizontal layer in two scenarios, wrench shear and transpression. By wrench shear we refer to a horizontally directed distributed simple shear on vertical shear planes (Sanderson 1982). The term transpression was first used by Harland (1971) in reference to the deformation caused by the oblique convergence of rigid plates. Sanderson & Marchini (1984) expanded the term to mean a zone of wrench (or transcurrent) shearing accompanied by horizontal shortening across the zone and vertical stretching. According to this usage, there is no stretch along the zone leading to extrusion of material at the ends.

The most obvious geologic example of instabilities arising in wrench shear is the formation of en échelon folds adjacent to strike-slip faults (Moody & Hill 1956, Wilcox *et al.* 1973, Harding 1974). An en échelon array consists of a series of folds with roughly parallel hinge lines oriented at a consistent angle to the associated strike-slip faults (Fig. 1). Numerous natural examples of en échelon fold systems are discussed by Moody & Hill (1956), Wilcox *et al.* (1973), Harding (1974), Graham (1978) and Little (1992), while experimental work has been done by Wilcox *et al.* (1973) and Odonne & Vialon (1983). Odonne & Vialon (1983) used analog models of simple shear to show that folds initiate with axes oriented close to 45° to the long dimension of the wrench zone. This observation is consistent with theoretical work proposing that folds initiate with axes normal to the axis of infinitesimal shortening in the layer (Flinn 1962, Treagus & Treagus 1981). Model experiments by Wilcox *et al.* (1973, p. 296) using simple shear boundary conditions showed that this angle is always less than 45° and may consistently be about 30°. In naturally occurring en échelon fold sets the angle between the hinges and the associated shear zone is usually less than 45° and may be less than 20° (Moody & Hill 1956, Wilcox *et al.* 1973).

Several explanations for this discrepancy between theory and observations have been proposed. First, in a rotational deformation such as simple shear, material lines will asymptotically rotate towards the shear direction. While fold hinges will not necessarily behave as

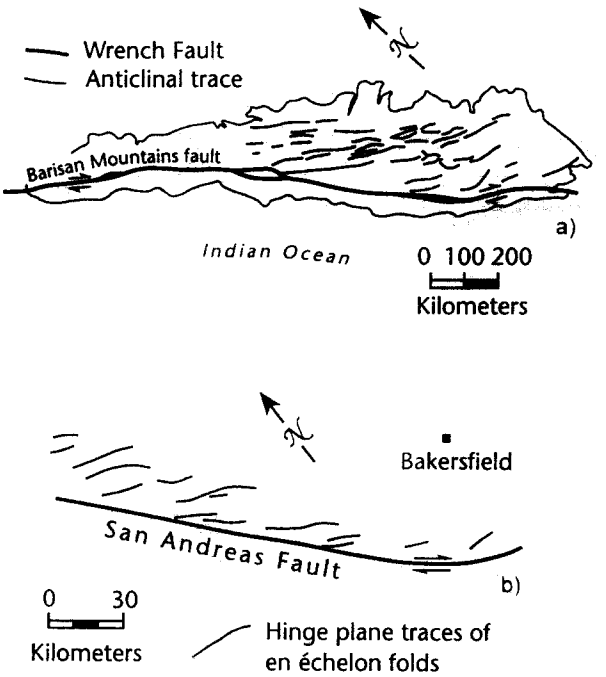

Fig. 1. En échelon fold systems developed adjacent to wrench faults. (a) Folds northeast of Barisan Mountains (Semangko) fault in Sumatra (from Wilcox *et al.* 1973). (b) Folds along the San Andreas fault in California (from Harding 1974).

material lines (Treagus & Treagus 1981), model work has shown that they will rotate in this type of deformation (Odonne & Vialon 1983). Thus, the angle between axes of en échelon folds and associated faults will decrease with continued deformation (Sanderson & Marchini 1984, Ridley 1986). If this is the case, as the angle lessens the fold will progressively tighten as strain accumulates perpendicular to the fold axis (Sanderson & Marchini 1984, Little 1992). Sanderson & Marchini (1984) showed that if an en échelon fold system initiates with axes at 45° to the associated shear zone, reduction of the angle to 22° necessitates a shear strain of $\gamma = 2$ and shortening normal to the fold hinge of 60%. They concluded that since this amount of shortening is seldom observed in natural en échelon fold systems, low angles between fold hinges and wrench faults is not due solely to rotation.

An alternative explanation is that en échelon fold systems initiate with hinges at lower angles to the shear plane due to transpression. This possibility has been treated theoretically by Sanderson & Marchini (1984), McCoss (1986) and Treagus & Treagus (1992). Sanderson & Marchini (1984) showed that additional shortening across a zone of wrench shear increases the angle between the minimum infinitesimal stretching direction and the shear plane; it follows that any folds will initiate at a lower angle to the zone boundaries. McCoss (1986) used a geometrical method to determine the orientation of the incremental shortening direction with respect to the boundaries of a transpressional zone; this method also demonstrated that added shortening increases the angle between incremental shortening and the shear plane.

With this work as motivation, we seek to demonstrate

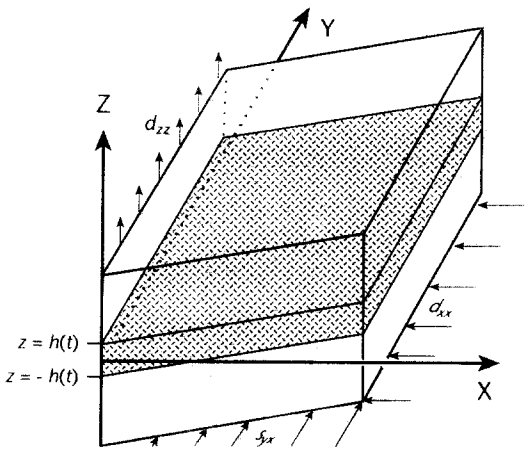

Fig. 2. The basic system examined in this paper. The layer has interfaces at $z = \pm h(t)$. The layer and medium are undergoing shear parallel to the y–z plane with the shear direction parallel to y. Superimposed on this is a pure shearing with the axis of maximum shortening parallel to x and axis of maximum stretching parallel to z.

the connection between the type of flow in the layer and the orientation of the resulting instabilities with the maximum growth rate. A linear stability analysis (which is limited to the onset of instabilities) is well suited to determining the initial orientation of fold axes in a wrench or transpressional deformation. Additionally, we point out that the theoretical studies mentioned above (e.g. Flinn 1962, Treagus & Treagus 1981, Sanderson & Marchini 1984, McCoss 1986) determine the orientations of fold axes by assuming that folds initiate with hinges at right angles to the infinitesimal shortening direction. While this may seem obvious, we rigorously test this assumption in a rotational deformation.

ONSET OF INSTABILITY IN A THREE-DIMENSIONAL LAYERED MEDIAN DURING TRANSPRESSIONAL DEFORMATION

Development of the model

To model a wrench- or transpressional-type deformation, we choose a co-ordinate system (x, y, z) consistent with the geologic characteristics of such zones; namely, a zone of deformation bounded by steeply dipping faults or shear zones (Sanderson & Marchini 1984). We choose the co-ordinates so that x is horizontal and perpendicular to the length of the zone, z is vertical, and y is parallel to the length of the zone.

A fluid system consisting of a single horizontal layer of fluid of thickness $\bar{H}$ (in dimensional variables) embedded in a less viscous medium is assumed to occupy the three-dimensional region described by our Cartesian system (Fig. 2). The mean position of the middle of the layer is at $z = 0$, and the mean positions of the interfaces are initially located at $\pm h(t)$ (in dimensionless variables), while perturbations from these mean positions are represented by $\zeta(x, y, t)$. We assume that the fluids are Newtonian with the viscosity of the layer denoted by μ and the upper and lower medium by μ'. Since quan-

tities associated with the layer are used for non-dimensionalization our assumption that the layer is more competent than its surroundings implies that the viscosity ratio $r = \mu'/\mu < 1$.

We use a linear stability analysis to determine the stability of the competent layer in the basic flow and to determine the orientation of any structures that result from instability. The governing equations of motion and the relevant interfacial conditions are given in the Appendix, as are most of the mathematical details. This technique follows the work of Ramberg (1959, 1963), Biot (1961, 1964), Smith (1975), Fletcher (1977, 1991) and others. Fletcher (1991) examined the three-dimensional stability of a viscous layer parallel to the x–y plane with the principal shortening direction parallel to x, the principal axis of extension parallel to z, and the axis of intermediate strain (either shortening or extension) parallel to y. Our analysis is similar to Fletcher's (1991) analysis; however, we examine the development of instabilities in a rotational deformation, whereas Fletcher examined an irrotational deformation with no component of shear strain parallel or perpendicular to the layer. It is also similar to the work of Benjamin & Mullin (1988), who examined the stability of a horizontal layer in what was effectively wrench shear. However, their analysis had an unconfined upper surface and was stress free at the lower interface. We also consider the stability of a pinch-and-swell disturbance since this type of structure is particularly sensitive to the basic flow.

Fletcher (1991) analyzed the fate of perturbations in the shape of the interface of the form $\zeta = \mathcal{A}(t) \cos(lx) \cos(my)$. From this analysis he concluded that a cylindrical disturbance is the most unstable disturbance; consequently we will examine the stability of a cylindrical disturbance of the form $\zeta = \mathcal{A}(t) \cos(\alpha x - \beta y)$. Although surface examples of en échelon folds tend to be doubly-plunging we use cylindrical geometry as a first approximation to an en échelon fold array. The angle, θ, between the fold axis and the y-axis is $\tan^{-1}(\beta/\alpha)$.

There are important differences between the geologic situations discussed previously and our simplistic model. The en échelon folds discussed earlier are generally (but not always) near-surface (or at-surface) phenomena, implying that there is no overlying medium and consequently the upper surface supports no shear stress. In contrast, our model has an overlying viscous medium which is appropriate for layers at some depth in the crust. In addition, while gravity may have an effect on growth rates, it has no effect on the orientation of horizontal structures and we neglect it in our model. We want to emphasize that surface wrench faulting or transpression is not the only environment where this type of strain is encountered. A wrench-type straining may occur at deeper levels in the crust; examples of wrench shear at lateral tips or ramps in thrust zones have been given (Coward & Potts 1983). Also, deformation at deeper levels in orogenic zones with significant components of wrench shear have been documented by Brun & Burg (1982) and Ridley (1986). Of course, a significant component of a wrench-type shear may occur within layers in shear zones if the layering is oriented obliquely to the shear plane and the intersection between layering and the shear plane is parallel to the length of the zone.

Basic flow associated with transpression

We require a basic flow that satisfies the criteria given above in terms of being a suitable model for deformation associated with wrench shear and transpression. From our choice of coordinates the determination of the basic flow is straightforward, consisting of shearing parallel to the y-axis, shortening parallel to x (perpendicular to the shear plane) and extension parallel to z (Fig. 2). According to Sanderson & Marchini (1984) and McCoss (1986) in a transpressional deformation no material is extruded or intruded from the ends of the zone, so the pure shear component of the deformation has no stretching (or shortening) parallel to the length of the zone. Although there are known examples of orogenic belts with large amounts of horizontal extension parallel to the length of the belt (Ellis & Watkinson 1987), we know of no work specifically documenting a large additional component of stretching (or shortening) parallel to the length of a transpressional zone. Should this latter scenario be considered transpression? In any case, it seems possible that this type of strain may occur on smaller scales and for generality our model allows for a pure shear component of stretching parallel to y. Most of our examples discussed later set this component to zero, although we also give an example with extension parallel to y.

The basic flow is denoted by $\mathbf{v}_0 = (u_0, v_0, w_0)$ and the strain rates parallel to x, y and z may be written as $\bar{D}_{xx}$, $\bar{D}_{yy}$ and $\bar{D}_{zz}$, respectively, and the shear strain rate parallel to y is $\bar{S}_{yx}$ (the overbars denote dimensional quantities). We then define appropriate dimensionless strain rates as $d_{ii} = \bar{D}_{ii}/\bar{e}$ for $i = x, y$ and z (no sum on i) and $s_{yx} = \bar{S}_{yx}/\bar{e}$. The term $1/\bar{e}$ is the scale factor for time given by $\bar{e} = (\mathbf{D}:\mathbf{D})^{1/2}$, where $\mathbf{D}$ is the rate-of-strain tensor of the imposed deformation. For constant d_{xx}, d_{yy}, d_{zz} and s_{yx} we then have $d_{xx} < 0$, $d_{zz} > 0$ and $d_{xx} < d_{yy} < d_{zz}$.

The basic velocity distribution for this deformation may be written as:

$$\mathbf{v}_0(x, y, z) = \mathbf{v}_0' = \mathbf{v}_0'' = (d_{xx}x, d_{yy}y + s_{yx}x, d_{zz}z), \quad (1)$$

where a prime indicates a quantity associated with the upper medium, a double prime indicates a quantity associated with the lower medium, and no subscript indicates a quantity associated with the layer. The velocity gradients tensor is:

$$\nabla\mathbf{v} = \begin{pmatrix} d_{xx} & 0 & 0 \\ s_{yx} & d_{yy} & 0 \\ 0 & 0 & d_{zz} \end{pmatrix} \quad (2)$$

with pure shear and simple shear components:

$$\nabla\mathbf{v}_{ps} = \begin{pmatrix} d_{xx} & 0 & 0 \\ 0 & d_{yy} & 0 \\ 0 & 0 & d_{zz} \end{pmatrix} \text{ and } \nabla\mathbf{v}_{ss} = \begin{pmatrix} 0 & 0 & 0 \\ s_{yx} & 0 & 0 \\ 0 & 0 & 0 \end{pmatrix} \quad (3)$$

respectively. This velocity distribution is an exact solution to the governing system of equations (A3)–(A5) and satisfies the interfacial conditions (A6) for planar interfaces.

Stability analysis

The purpose of this analysis is to determine how the shape of the layer evolves with time, i.e. if folds and/or pinch-and-swell structures (boudins) develop. To this end, it is the stability or instability of the viscous layer in the basic flow that will be considered in the analysis. This is accomplished through use of a linear stability analysis to determine the fate of infinitesimal perturbations in the shape of the layer. A perturbation may be defined as infinitesimal when the deviation of an interface from a planar shape δ is very small in comparison with the thickness of the layer $\bar{H}$, i.e. $\varepsilon = \delta/\bar{H} \ll 1$. These small variations in the shape of the interfaces result in slight perturbations of the basic velocity field. Because the perturbations are small the total flow may be separated as

$$\mathbf{v} = \mathbf{v}_0 + \varepsilon\mathbf{v}_1 + O(\varepsilon^2), \tag{4}$$

where $\varepsilon\mathbf{v}_1 + O(\varepsilon^2)$ is the flow generated from the instability. Since $\varepsilon \ll 1$, higher order terms of ε (i.e. $O(\varepsilon^2)$) are neglected to make the analysis linear. It is assumed that perturbations with all orientations in the horizontal plane are present—all, however, are infinitesimal. The disturbance flow must satisfy the governing system of equations (A3)–(A5) and the interfacial conditions (A6) independently of the basic flow.

As discussed above, we examine the stability of the layer to cylindrical fold-like perturbations of the form $\zeta(x, y, t) = \mathcal{A}(t) \cos(\alpha x - \beta y)$, where $\mathcal{A}(t)$ is the amplitude of the disturbance and ζ is of order ε. Because the interface is a material surface of discontinuity lines of equal phase (e.g. fold hinges) will deform in the basic flow; consequently the (dimensional) wavenumbers α and β are functions of time. Although long-term effects are beyond the scope of this linear analysis, satisfaction of the kinematic boundary condition (A6a) requires proper formulation of the time-dependent effects of the wavenumbers. For the purposes of this analysis we assume that the fold hinges behave as material lines. Thus, perturbations are described by solutions of the form:

$$\begin{aligned}\zeta(x, y, t) &= \mathcal{A}(t) \cos(\alpha_1 x - \beta(y - Sxt)) \\ &= \mathcal{A}(t) \cos(\alpha z - \beta y),\end{aligned} \tag{5}$$

where

$$\alpha = \alpha_1 + \beta St. \tag{6}$$

Equation (5) describes a surface with periodic cylindrical fold-like forms with lines of constant phase at an angle θ to the y-axis. The wavenumbers α and β are parallel to x and y, respectively, and ω is the wavenumber perpendicular to the wave crests, so $\omega^2 = \alpha^2 + \beta^2 > 0$ (Benjamin & Mullin 1988). The angle between ω and the x-axis (θ) is $\tan^{-1}(\beta/\alpha)$. Figure 3 shows these relationships, where lines of constant phase (such as fold hinges) initially at some arbitrary angle to the shear plane will rotate from their initial positions, shown by the solid lines, to positions shown by the dashed lines (the amount of rotation is grossly exaggerated) after some time t.

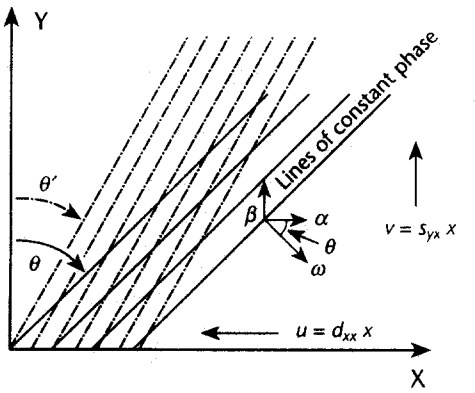

Fig. 3. Lines of constant phase (e.g. fold hinges) in the x–y plane. Wave vectors α and β (parallel to the x- and y-axes, respectively) and the resultant ω (equal to $\sqrt{\alpha^2 + \beta^2}$ and perpendicular to the lines of constant phase) are shown. θ is the angle between ω and the x-axis (as well as the lines of constant phase and the y-axis). The shear component of the basic flow will cause the lines to rotate from the positions shown by solid lines, while the shortening component will cause the lines to move closer together with time. The amount of rotation shown is grossly exaggerated. After Benjamin & Mullin (1988).

The fundamental purpose of a stability analysis is to determine how the amplitude of the disturbances, $\mathcal{A}$, changes with time, i.e. to determine the value of $\mathrm{d}\mathcal{A}(t)/\mathrm{d}t$. The system of equation (A26) resulting from the stability analysis represents an eigenvalue problem for the quantity $[1/\mathcal{A}\ \mathrm{d}\mathcal{A}/\mathrm{d}t]$. Solution of this system results in the secular relation:

$$\frac{\mathrm{d}\mathcal{A}}{\mathrm{d}t} = \mathcal{A}\left(d_{zz} + \frac{(1 - r)(k^2 d_{zz} - l^2 d_{xx} - m^2 d_{yy} + lms_{yx})}{k(k(r^2 - 1) + (1 + r^2)\sinh k + 2r\cosh k)}\right). \tag{7}$$

We may write this as:

$$\frac{\mathrm{d}\mathcal{A}}{\mathrm{d}t} = a_1\mathcal{A}, \tag{8}$$

where a_1 is the growth rate:

$$a_1 = d_{zz} + \frac{(1 - r)(k^2 d_{zz} - l^2 d_{xx} - m^2 d_{yy} + lms_{yx})}{k(k(r^2 - 1) + (1 + r^2)\sinh k + 2r\cosh k)}, \tag{9}$$

$k = 2\omega h = 2\pi/\lambda\bar{H}$ is the dimensionless wavenumber of the disturbance associated with the dimensionless wavelength λ/H, and l and m are the dimensionless wavenumbers parallel to the x-axis and y-axis given by αh and βh, respectively. Note that $k^2 = l^2 + m^2$.

Because the system of basic equations (A3)–(A5) and interfacial conditions (A6) are valid only for infinitesimal perturbations, our analysis is restricted to a suf-

ficiently small period in dimensional time that changes in λ and H are negligible relative to the scale factor for time, $1/\bar{e}$. Therefore, at the onset of instability k may be treated as a constant, and we adopt the criteria whereby the instability, stability, or neutral stability of the layer to buckling is determined by whether a_1 is positive, negative, or zero, respectively, for all time t. We therefore treat a_1 as the instantaneous growth rate of a buckling disturbance. The secular relation (7) is a more generalized form of Fletcher's (1991) equation (29) since it includes the effects of wrench shear on the system; this is represented by the term lms_{yx}.

Pinch-and-swell mode

A full description of the evolution of the shape of the layer also requires consideration of the symmetric pinch-and-swell mode of instability. A similar analysis (see the Appendix) for a symmetric pinch-and-swell perturbation yields the growth rate b_1 of a pinch-and-swell disturbance:

$$b_1 = d_{zz} - \frac{(1-r)(k^2 d_{zz} - l^2 d_{xx} - m^2 d_{yy} + lms_{yx})}{k(k(r^2-1) + (1+r^2)\sinh k + 2r\cosh k)}. \quad (10)$$

Here b_1 is the growth rate for a symmetric disturbance:

$$\zeta(x, y, t) = I\mathcal{B}(t)\cos(\alpha x - \beta y). \quad (11)$$

Again, since we are limited to the onset of instability we adopt a stability criteria similar to that discussed above where the stability, neutral stability, or instability of a pinch-and-swell disturbance is indicated by $b_1 < 0$, $b_1 = 0$, or $b_1 > 0$, respectively.

DISCUSSION

For all values of l and $m > 0$ and values of $r < 1$, a_1 is positive and the layer is identically unstable to fold-type perturbations. Since there is no critical value where a_1 is positive for only a single value of k, we will characterize the wavelength of the resulting instability by the classical method of determining which wavenumber has the largest growth rate (Drazin & Reed 1981). Thus the dominant wavenumber is given by the relation:

$$\frac{\partial a_1}{\partial l} = \frac{\partial a_1}{\partial m} = 0. \quad (12)$$

By solving this relation numerically a graph of the dominant wavelength-to-thickness ratio may be plotted as a function of the viscosity ratio r (Fig. 4). The dominant wavenumber is independent of the strain parameters d_{xx}, d_{yy}, d_{zz} and s_{yx}, and is only a function of the viscosity ratio r and is in fact the same as those reported by Smith (1975) and Fletcher (1977, 1991) and for two- and three-dimensional cases. This latter result is not surprising since our results must reduce to the appropriate two- and three-dimensional results given

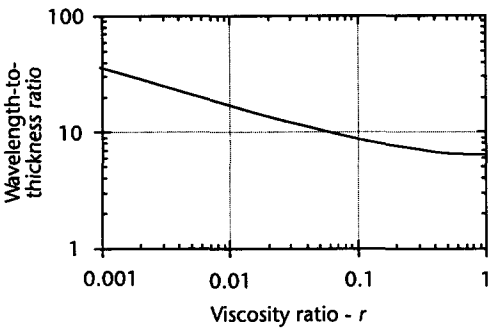

Fig. 4. Graph of the dominant wavelength-to-thickness ratios for a buckling disturbance at the onset of instability as a function of the viscosity ratio r.

the proper strain parameters. We now turn to our main focus, the orientation of the resulting structures.

We want to determine the orientation of the disturbances with the maximum growth rate. Using equation (12) above to find the maximum of a_1 as a function of l and m, the orientation (θ) of the dominant wavelength is found using $\theta = \tan^{-1}(m/l)$. Figure 5 shows contour plots of the instantaneous growth rate a_1 vs wavenumbers l (ordinate) and m (abscissa) for four specific cases: Fig. 5(a) is for wrench shear alone ($d_{xx} = d_{yy} = d_{zz} = 0$ and $s_{yz} = \sqrt{2}$); Fig. 5(b) shows a_1 for transpression where the rate of shortening parallel to x (due to the pure shear component of the deformation) is half that of the rate of shear parallel to y ($d_{zz} = -d_{xx} = 1/2s_{yx}$); Fig. 5(c) shows a_1 for transpression with rate of shortening equal to the rate of shear ($d_{zz} = -d_{xx} = s_{yx}$); Fig. 5(d) shows an example where the pure shear component of the deformation has the axis of shortening parallel to x and extension parallel to y, not z ($d_{yy} = -d_{xx} = s_{yx}$). This last example is not true transpression, but since this type of strain may occur on a smaller scale we include an example of it here. From these plots the values of m and l corresponding to the maxima of a_1 may easily be read off; for example, in Fig. 5(b) $l = 0.323$ and $m = 0.199$ so $\tan^{-1}(0.199/0.323) \approx 32°$. The maxima in Figs. 5(a), (c) & (d) correspond to the initiation of fold hinges at approximately 45°, 23° and 13° to the y-axis, respectively. This will be discussed further below.

When $s_{yx} \neq 0$ and $d_{xx} = d_{yy} = d_{zz} = 0$, the layer is identically unstable to pinch-and-swell perturbations for all values of $l > 0$ and $m < 0$ and values of $r < 1$. As before, since there is no critical value where b_1 is positive for only a single value of k, we characterize the wavelength of the resulting instability according to which wavenumber has the largest growth rate. Figure 5(e) shows a contour plot of b_1, vs wavenumbers l and m for wrench shear ($d_{xx} = d_{yy} = d_{zz} = 0$ and $s_{yx} = \sqrt{2}$). The maximum in this plot corresponds to the formation of boudin hinges at 135° to the positive y-axis.

Folds and boudinage in wrench shear

For wrench shear the parameters used are $d_{xx} = d_{yy} = d_{zz} = 0$ and $s_{yx} = \sqrt{2}$. In this case the axes of the buckling disturbance with the maximum growth rate are initially oriented at 45° to the shear plane (Fig. 5a), which is

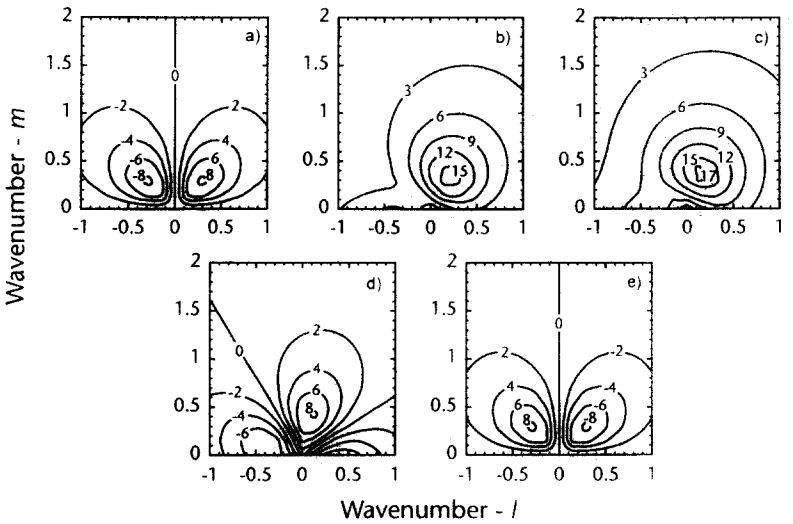

Fig. 5. Contours of the growth rate a_1 of a fold-like disturbance as a function of the wavenumbers l (parallel to the x-axis) and m (parallel to the y-axis) for a layer with viscosity ratio $r = 0.01$ (layer 100 times more viscous than the surrounding medium). The angle between the hinge of the fastest growing disturbance and the y-axis is given by the ratio m/l of the maximum. (a) Plot of a_1 for wrench shear ($d_{xx} = d_{yy} = d_{zz} = 0$ and $s_{yx} = \sqrt{2}$). (b) Plot of a_1 for transpression with the rate of shortening half that of the rate of shear ($d_{zz} = -d_{xx} = 1/2\ s_{yx}$). (c) Plot of a_1 for transpression with the rate of shortening equal to the rate of shear ($d_{zz} = -d_{xx} = s_{yx}$). (d) Plot of a_1 for axis of shortening parallel to x and extension parallel to y, not z ($d_{yy} = -d_{xx} = s_{yx}$). (e) Plot of b_1 for a pinch-and-swell disturbance in wrench shear ($d_{xx} = d_{yy} = d_{zz} = 0$ and $s_{yx} = \sqrt{2}$).

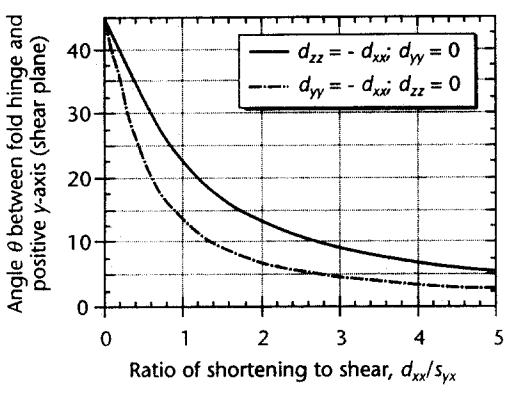

Fig. 6. The angle θ between the hinge of the fastest growing buckling disturbance and the y-axis as a function of the ratio of shortening parallel to the x-axis, d_{xx}, to the shear parallel to y, s_{yx}. Curves are shown corresponding to extension parallel to z alone and parallel to y alone.

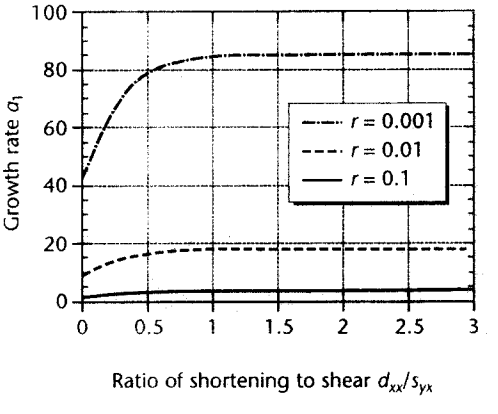

Fig. 7. Dimensionless growth rates as a function of the ratio of shortening across the shear plane, d_{xx}, to shear, s_{yx} with $d_{zz} = -d_{xx}$. Three curves are shown for viscosity ratios of $r = 0.1$, $r = 0.01$ and $r = 0.001$.

normal to the minimum infinitesimal stretching direction in the layer. Additionally, the axes are initially parallel to the maximum infinitesimal stretching direction and thus some component of extension parallel to the fold axes will occur.

The extensional strain is responsible for the instability of pinch-and-swell disturbances in the layer, which have axes oriented at 135° to the positive y-axis (at right angles to the fold axes). The dimensionless growth rates for pinch-and-swell instabilities are much smaller (of the order of 0.33 for $r = 0.01$) than the dimensionless growth rates for fold-type disturbances (8.7) and growth of these disturbances may be weak.

Folding and boudinage in transpression

Recalling that for $d_{xx} < 0$, $d_{zz} > 0$ and $s_{yx} \neq 0$, the deformation falls within the definition of transpression discussed earlier. Figure 6 shows the angle θ as a function of the ratio of shortening (d_{xx}) to shear (s_{yz}) for the two cases of $d_{xx} = -d_{zz}$ and $d_{xx} = -d_{yy}$. The angle of initiation is independent of the competence contrast. As the ratio of shortening to shear increases the angle between the fold hinges and the y-axis decreases; in other words, transpression will cause the fold axes to initiate at less than 45° to the shear direction. The buckles do initiate with axes normal to the minimum infinitesimal stretching direction in the layer, and our results confirm the prevailing views in the literature (Flinn 1962, Treagus & Treagus 1981, Sanderson & Marchini 1984, McCoss 1986). It is worth noting that in the case where $d_{zz} = 0$ (no vertical extension) and $d_{yy} > 0$, folds initiate with axes at much lower angles to the shear plane; for example, if the rate of shortening is equal to the rate of shear ($|d_{xx}/s_{yx}| = 1$) and all extension is parallel to y, folds will nucleate at 13°; if all extension is parallel to z, folds will nucleate at 23°.

Figure 7 shows the growth rate a_1 as a function of the

ratio of shortening, d_{xx}, to shear, s_{yx}, for $d_{xx} = -d_{zz}$ and $r = 0.1$, 0.01 and 0.001. The growth rates of fold-type disturbances in wrench shear are relatively low in comparison to those where there is extension parallel to z; as d_{zz} increases the growth rate increases significantly due to the added kinematic growth effects. For example, for a viscosity ratio of 0.01 (layer 100 times more viscous than the medium) the non-dimensionalized growth rate is approximately 8.7 for wrench shear (at the y-intercept), whereas it is over 18 for a two-dimensional case with shortening parallel to the layer and extension normal to the layer. As d_{zz} increases relative to s_{yz}, the growth rate asymptotically approaches this latter value. This theoretical result is borne out by the model experiments of Wilcox *et al.* (1973) where small angles of convergence resulted in much more pronounced fold growth than wrench shear alone. We note that the strain distribution in a folded rock will be different if the folds formed in a wrench shear environment (due to lower amplification rates) than if they formed in a situation where extension occurred normal to the layer.

The growth rate b_1 for pinch-and-swell structures decreases as d_{zz} increases since the basic flow opposes the growth of the instability (Smith 1975). We emphasize, however, that in wrench shear and for small values of d_{zz}/s_{yx} that the growth rate is greater than zero and these disturbances are unstable. This is due to the fact that with d_{zz} sufficiently small, the dynamic growth rate is larger than the opposing kinematic deamplification. When $d_{zz} = 0$ there are, of course, no competing kinematic effects. Smith (1975, 1977) found that the growth rates of pinch-and-swell structures in a two-dimensional deformation were negative and concluded that such structures would not grow in layered Newtonian fluids. Smith (1977) invoked non-Newtonian (specifically strain-rate softening) behavior as a condition for the growth of pinch-and-swell structures. Our analysis shows that these structures can develop in layered Newtonian fluids due to three-dimensional effects and are thus not proof of non-Newtonian behavior. We note further that the instability of pinch-and-swell structures does not require a component of simple shear. In the case where there is no wrench shear ($s_{yz} = 0$) and the layer is subjected to pure shear with extension parallel to y, pinch-and-swell disturbances with axes parallel to x are unstable. The full three-dimensional geometry of the deformation must be taken into account when examining geologic structures!

Extensional features parallel to fold hinges have been documented in en échelon fold systems by Little (1992). Pinch-and-swell structures have not yet been specifically documented in natural en échelon occurrences, nor have they been documented in experimental work (Wilcox *et al.* 1973, Brun & Burg 1982, Odonne & Vialon 1983, Coward & Potts 1984, Ridley 1986). However, both conjugate fault sets and tension gashes at high angles to the fold hinges are commonly reported by workers studying natural en échelon fold systems. Similar structures were reported in the model experiments by Wilcox *et al.* (1973), p. 304), who reported that tension gashes cross the en échelon fold axes at right angles. The presence of these structures rather than boudinage may result from the rheologic behavior of upper crustal rocks and the materials used in modeling experiments, which tend to behave in a brittle fashion during extension. In some environments, such as within ductile shear zones, it seems possible that boudins may form if layering is oriented such that the layer undergoes a sufficient degree of wrench strain.

Comments on finite growth effects

A topic of current interest is the behavior of fold axes in a rotational deformation such as transpression. While this analysis cannot make quantitative predictions on the long-term development of finite amplitude folds, we discuss some qualitative aspects of fold rotation from the perspective of this analysis. There are two general models of the behavior of fold hinges in a rotational deformation. The first assumes that fold hinges, after initiation, behave passively and simply rotate as material lines in the flow (Flinn 1962, Sanderson & Marchini 1984). The second model assumes that fold hinges remain perpendicular to the axis of maximum finite shortening in the layer (Treagus & Treagus 1981, 1992). Treagus & Treagus (1981) make the argument, which we believe to be valid, that the effects of competence contrasts do not suddenly vanish after folds initiate. They argue further that any 'increment' of buckling is perpendicular to the incremental shortening direction in the layer (what constitutes an increment of buckling is not specified). Thus, each successive increment of buckling is oblique (by a small angle) to the previous increment and the resulting finite amplitude fold is the sum of all the non-coaxial increments, with an axis perpendicular to the axis of maximum finite shortening in the layer. In this model it is necessary that the fold hinge undergoes some degree of migration (Treagus & Treagus 1981, 1992).

While we believe this to be a better model of fold development in a rotational system than one which assumes only passive rotation, there are several possible effects it ignores. First, leaving aside the question of when an infinitesimal fold can be considered finite in amplitude, the growing fold will modify the basic flow in some local area by its presence. One effect of this modification may be a 'bending' of the streamlines in the neighborhood of the fold, resulting in a local rotation of the principal axis of infinitesimal shortening. Consequently each following increment of buckling, while perpendicular to the local incremental shortening direction, may not be perpendicular to the overall, or 'average', incremental shortening direction in the layer. This 'corrugation effect' of the fold hinges (Troitsky 1976) may result in an anisotropy that causes partitioning of strain with components of shortening normal to fold hinges and shearing parallel to the fold hinges (Goguel 1962, Cobbold & Watkinson 1981, Watkinson & Cobbold 1981). Second, since the interaction of each increment of folding with a finite amplitude fold is a non-

linear process the addition of each increment is not straightforward.

A non-linear analysis that examines the effects of the higher-order terms neglected in this analysis is necessary to determine the consequences of these effects. A non-linear analysis along the lines of the classic work of Stuart (1960) and Watson (1960) (a weakly non-linear stability analysis) may not be applicable to this model, however. An analysis of their type makes the necessary assumption that only a *single* unstable wavenumber (the critical wavenumber) becomes unstable at some point, instead of the continuous and virtually infinite spectrum of unstable wavenumbers present in this analysis. Furthermore, an analysis of this type requires that the growth rate of the disturbance, a_1, be sufficiently close to the curve of marginal stability so that a_1 is of the order $O(\varepsilon^2)$ (i.e. $0 < a_1 \ll 1$) to ensure that an asymptotic expansion of the amplitude equation resulting from the kinematic boundary condition (A6a) is both valid and appropriate. Since there is no state of marginal stability in this problem (except for the uninteresting case of no deformation) and $a_1 \gg 1$, other approaches must be examined (Drazin & Reid 1981, p. 378).

Experimental models will undoubtedly be of benefit in understanding these processes. Unfortunately, as pointed out by Treagus & Treagus (1992) the angular difference between the axis of finite extension in a layer undergoing shearing and the material line parallel to the initial axis of buckling may be only 1° or 2°. The model work of Odonne & Vialon (1983) had a spread of 15–20° of the orientation of the initial fold hinges. Furthermore, an infinitesimal amplitude fold is difficult to see, making determination of the initial axial orientations difficult. Nonetheless, many important questions may be answered. Numerical models, such as those using finite elements, will also undoubtedly be helpful in answering some of these questions.

CONCLUSIONS

The main results of this analysis are as follows.

(1) In a rotational deformation, folds initiate with axes normal to the minimum infinitesimal stretching direction in the layer. In wrench shear the fastest growing buckling disturbances form with axes at 45° to the shear direction. Disturbances with axes at 90° to the fold hinges are also unstable. The formation of pinch-and-swell structures does not require non-Newtonian behavior. Transpression, resulting from an added component of shortening normal to the shear plane, causes folds to initiate at a smaller angle to the shear plane and also results in larger growth rates of folding instabilities. This angle is only a function of the relative magnitudes of the principal strain rates and is not a function of the viscosity of the layer.

(2) The bulk strain of a deforming system exerts a strong controlling influence on not only the orientation of the dominant structures, but also on the type of structures which are produced. To date it has been assumed that the principal governing factors for the initiation of folds or boudins in layered rocks is the competence contrast between the layer and medium and whether the strain is layer parallel shortening or extension. This analysis shows that the bulk flow is an additional important variable.

Acknowledgements—We would like to thank Dr David J. Wollkind for providing many helpful suggestions during the course of this work. Helpful reviews by Sue Treagus and Ray Fletcher also greatly improved the manuscript.

REFERENCES

Alexander, J. I. D. 1981. Folds and folding in single- and multi-layered rocks: mathematical models and field observations. Unpublished Ph.D. dissertation, Washington State University, Washington.

Benjamin, T. B. & Mullin, T. 1988. Buckling instabilities in layers of viscous liquid subjected to shearing. *J. Fluid Mech.* **195**, 523–540.

Biot, M. A. 1957. Folding instability of a layered viscoelastic medium under compression. *Proc. R. Soc. Lond.* **A242**, 444–454.

Biot, M. A. 1959. On the instability of folding deformation of a layered viscoelastic medium under compression. *J. Appl. Mech.* **26**, 393–400.

Biot, M. A. 1961. Theory of folding of stratified viscoelastic media and its implications in tectonics and orogenesis. *Bull. geol. Soc. Am.* **72**, 1595–1620.

Biot, M. A. 1964. Theory of viscous buckling of multilayered fluids undergoing finite strain. *Phys. Fluids* **7**, 855–859.

Brun, J. P. & Burg, J. P. 1982. Combined thrusting and wrenching in the Ibero-Amorican arc: a corner effect during continental collision. *Earth Planet. Sci. Lett.* **61**, 319–332.

Cobbold, P. R. & Watkinson, A. J. 1981. Bending anisotropy: a mechanical constraint on the orientation of fold axes in an anisotropic medium. *Tectonophysics* **72**, T1–T10.

Coward, M. P. & Potts, G. J. 1983. Complex strain patterns developed at the frontal and lateral tips to shear zones and thrust zones. *J. Struct. Geol.* **5**, 383–399.

Drazin, P. G. & Reid, W. H. 1981. *Hydrodynamic Stability*. Cambridge University Press, New York.

Ellis, M. A. & Watkinson, A. J. 1987. Orogen-parallel extension and oblique tectonics: The relation between stretching lineations and relative plate motions. *Geology* **15**, 1022–1026.

Fletcher, R. C. 1977. Folding of a single viscous layer: Exact infinitesimal amplitude solution. *Tectonophysics* **39**, 593–606.

Fletcher, R. C. 1982. Analysis of the flow in layered fluids at small, but finite, amplitude with application to mullion structures. *Tectonophysics* **81**, 51–66.

Fletcher, R. C. 1991. Three-dimensional folding of an embedded viscous layer in pure shear. *J. Struct. Geol.* **13**, 87–96.

Flinn, D. 1962. On folding during three-dimensional progressive deformation. *Q. J. geol. Soc. Lond.* **118**, 385–433.

Goguel, J. 1962. *Tectonics* (English translation). Freeman and Co., London.

Graham, R. H. 1978. Wrench faults, arcuate fold patterns and deformation in the southern French Alps. *Proc. Geol. Ass.* **89**, 125–143.

Harding, T. P. 1974. Petroleum traps associated with wrench faults. *Bull. Am. Ass. Petrol. Geol.* **58**, 1290–1304.

Harland, W. B. 1971. Tectonic transpression in Caledonian Spitsbergen. *Geol. Mag.* **108**, 27–42.

Johnson, A. M. & Pfaff, J. 1989. Parallel, similar, and constrained folds. *Engng Geol.* **27**, 115–180.

Little, T. A. 1992. Development of wrench folds along the Border Ranges fault system, southern Alaska, U.S.A. *J. Struct. Geol.* **14**, 343–359.

McCoss, A. M. 1986. Simple constructions for deformation in transpression/transtension zones. *J. Struct. Geol.* **8**, 715–718.

Moody, J. D. & Hill, M. J. 1956. Wrench fault tectonics. *Bull. geol. Soc. Am.* **67**, 1207–1246.

Odonne, F. & Vialon, P. 1983. Analogue models of folds above a wrench fault. *Tectonophysics* **99**, 31–46.

Ramberg, H. 1959. Evolution of ptygmatic folding. *Norsk geol. Tidsskr.* **39**, 99–151.

Ramberg, H. 1962. Contact strain and folding instability of a multilayered body under compression. *Geol. Rdsch.* **51**, 405–439.

Ramberg, H. 1963. Fluid dynamics of viscous buckling applicable to folding of layered rocks. *Bull. Am. Ass. Petrol. Geol.* **47**, 484–505.
Ramberg, H. 1970a. Folding of laterally compressed multilayers in the field of gravity: Part I. *Phys. Earth & Planet. Interiors* **2**, 203–232.
Ramberg, H. 1970b. Folding of laterally compressed multilayers in the field of gravity: Part II. *Phys. Earth & Planet. Interiors* **4**, 83–120.
Ridley, J. 1986. Parallel stretching lineations and fold axes oblique to a shear displacement direction—a model and observations. *J. Struct. Geol.* **8**, 647–653.
Sanderson, D. J. 1982. Models of strain variation in nappes and thrust sheets: A review. *Tectonophysics* **88**, 201–233.
Sanderson, D. J. & Marchini, W. R. D. 1984. Transpression. *J. Struct. Geol.* **6**, 449–458.
Smith, R. B. 1975. Unified theory of the onset of folding, boudinage, and mullion structure. *Bull. geol. Soc. Am.* **86**, 1601–1609.
Smith, R. B. 1977. Formation of folds, boudinage, and mullion in non-Newtonian materials. *Bull. geol. Soc. Am.* **88**, 312–320.
Stuart, J. T. 1960. On the non-linear mechanics of wave disturbances in stable and unstable parallel flows. Part 1. The basic behavior in plane Poiseuille flow. *J. Fluid Mech.* **9**, 353–370.
Treagus, J. E. & Treagus, S. H. 1981. Folds and the strain ellipsoid: a general model. *J. Struct. Geol.* **3**, 1–17.
Treagus, J. E. and Treagus, S. H. 1992. Transected folds and transpression: how are they related? *J. Struct. Geol.* **14**, 361–367.
Treagus, S. H. 1973. Buckling stability of a viscous single-layer system, oblique to the principal compression. *Tectonophysics* **19**, 271–289.
Troitsky, M. S. 1976. *Stiffened Plates—Bending, Stability and Vibrations*. Elsevier, Amsterdam.
Watson, J. 1960. On the non-linear mechanics of wave disturbances in stable and unstable parallel flows. Part 2. The development of a solution for plane Poiseuille flow and for plane Couette flow. *J. Fluid Mech.* **9**, 371–389.
Watkinson, A. J. & Cobbold, P. R. 1981. Axial directions of folds in rocks with linear/planar fabrics. *J. Struct. Geol.* **3**, 211–217.
Wilcox, R. E., Harding, T. P. & Seely, D. R. 1973. Basic wrench tectonics. *Bull. Am. Ass. Petrol. Geol.* **57**, 74–96.
Wollkind, D. J. & Alexander, J. I. D. 1982. Kelvin–Helmholtz instability in a layered Newtonian fluid model of the geological phenomenon of rock folding. *SIAM J. Appl. Math.* **42**, 1276–1295.

APPENDIX

Governing equations and interfacial conditions

The general problem requires determination of the stability of a fluid that is stratified by viscosity and is immiscible. The fluids are assumed to be Newtonian and interfacial forces and density differences between the layers are ignored. The system consists of a single horizontal layer of a viscous fluid of thickness $\bar{H}$ (in dimensional variables) embedded in a less viscous medium with the interfaces of the layer perpendicular to the z-axis. The mean positions of the interfaces are located at $\pm h(t)$ (in dimensionless variables) while deviations from these mean positions are represented by $\zeta(x, y, t)$. Additionally, $\mathbf{v} = \mathbf{v}(x, y, z, t) = (u, v, w)$ are the velocity components, $p = p(x, y, z, t) = p^* + \rho_0 \mathbf{g} z$ is the reduced pressure where p^* is the total pressure, $\mu \equiv$ viscosity coefficient, $\mu/\rho_0 \equiv \nu \equiv$ kinematic viscosity, and $\mathbf{g} \equiv$ acceleration due to gravity. The bulk quantities of the upper and lower fluid region are denoted by a primed and double primed superscript, respectively, while those of the layer have no superscript.

All independent and dependent variables are considered in dimensionless form, and $\bar{H}$, $1/\bar{e}$, $\bar{e}\bar{H}$, $\mu\bar{e}$ and δ are the scale factors for distance, time, velocity, pressure and deviation of the interface from its mean position, respectively. Additionally, the following dimensionless parameters are used for the deviation of the interface from a plane and the viscosity ratio:

$$\varepsilon = \frac{\delta}{\bar{H}}, \qquad r = \frac{\mu'}{\mu}, \tag{A1}$$

respectively. The equation for the position of the interfaces may then be written as:

$$z = \pm h(t) + \varepsilon\zeta(x, y, t), \qquad \text{where } \lim_{l\to\infty} \frac{1}{2l}\int_{-l}^{l} \zeta(x, y, t)\mathrm{d}x = 0. \tag{A2}$$

In dimensionless variables, the governing Navier–Stokes equations of motion for a quasi-static, isotropic, isothermal single phase fluid of constant density in the upper medium, layer, and lower medium are, respectively:

$$\nabla \cdot \mathbf{v}' = 0, \qquad -\nabla p' + \mu\nabla^2\mathbf{v}' = 0 \tag{A3a–d}$$

$$\nabla \cdot \mathbf{v} = 0, \qquad -\nabla p + \mu\nabla^2\mathbf{v} = 0. \tag{A4a–d}$$

$$\nabla \cdot \mathbf{v}'' = 0, \qquad -\nabla p'' + \mu''\nabla^2\mathbf{v}'' = 0. \tag{A5a–d}$$

For $z = h(t) + \varepsilon\zeta(x, y, t)$ (at the upper interface), the following conditions apply:

$$w = \frac{\partial h}{\partial t} + \varepsilon\left(\frac{\partial\zeta}{\partial t} + u\frac{\partial\zeta}{\partial x} + v\frac{\partial\zeta}{\partial y}\right) \tag{A6a}$$

$$w' - \varepsilon u'\frac{\partial\zeta}{\partial x} - \varepsilon v'\frac{\partial\zeta}{\partial y} = w - \varepsilon u\frac{\partial\zeta}{\partial x} - \varepsilon v\frac{\partial\zeta}{\partial y} \tag{A6b}$$

$$\begin{aligned} -p' + 2\mu'\Big\{&\varepsilon^2\frac{\partial u'}{\partial x}\zeta_x^2 + \varepsilon^2\left(\frac{\partial u'}{\partial y} + \frac{\partial v'}{\partial x}\right)\zeta_x\zeta_y - \varepsilon\left(\frac{\partial u'}{\partial z} + \frac{\partial w'}{\partial x}\right)\zeta_x + \varepsilon^2\frac{\partial v'}{\partial y}\zeta_y \\ &-\varepsilon\left(\frac{\partial v'}{\partial z} + \frac{\partial w'}{\partial y}\right)\zeta_y + \frac{\partial w'}{\partial z}\Big\}\Big/(1 + \varepsilon^2\zeta_x^2 + \varepsilon^2\zeta_y^2) \\ = -p + 2\mu\Big\{&\varepsilon^2\frac{\partial u}{\partial x}\zeta_x^2 + \varepsilon^2\left(\frac{\partial u}{\partial y} + \frac{\partial v}{\partial x}\right)\zeta_x\zeta_y - \varepsilon\left(\frac{\partial u}{\partial z} + \frac{\partial w}{\partial x}\right)\zeta_x + \varepsilon^2\frac{\partial v}{\partial y}\zeta_y \\ &-\varepsilon\left(\frac{\partial v}{\partial z} + \frac{\partial w}{\partial y}\right)\zeta_y + \frac{\partial w}{\partial z}\Big\}\Big/(1 + \varepsilon^2\zeta_x^2 + \varepsilon^2\zeta_y^2) \end{aligned} \tag{A6c}$$

$$\begin{aligned} 2\mu'\Big\{&-\varepsilon\frac{\partial u'}{\partial x}\zeta_x - \varepsilon\frac{1}{2}\left(\frac{\partial u'}{\partial y} + \frac{\partial v'}{\partial x}\right)\zeta_y + \varepsilon\frac{1}{2}\left(\frac{\partial u'}{\partial z} + \frac{\partial w}{\partial x}\right)(1 - \varepsilon^2\zeta_x^2) \\ &-\varepsilon^2\frac{1}{2}\left(\frac{\partial v'}{\partial z} + \frac{\partial w'}{\partial y}\right)\zeta_x\zeta_y + \varepsilon\frac{\partial w'}{\partial z}\zeta_x\Big\} \\ = 2\mu\Big\{&-\varepsilon\frac{\partial u}{\partial x}\zeta_x - \varepsilon\frac{1}{2}\left(\frac{\partial u}{\partial y} + \frac{\partial v}{\partial x}\right)\zeta_y + \varepsilon\frac{1}{2}\left(\frac{\partial u}{\partial z} + \frac{\partial w}{\partial x}\right)(1 - \varepsilon^2\zeta_x^2) \\ &-\varepsilon^2\frac{1}{2}\left(\frac{\partial v}{\partial z} + \frac{\partial w}{\partial y}\right)\zeta_x\zeta_y + \varepsilon\frac{\partial w}{\partial z}\zeta_x\Big\} \end{aligned} \tag{A6d}$$

$$\begin{aligned} 2\mu'\Big\{&-\varepsilon^3\frac{\partial u'}{\partial x}\zeta_x^2\zeta_y - \varepsilon^3\frac{1}{2}\left(\frac{\partial u'}{\partial y} + \frac{\partial v'}{\partial x}\right)\zeta_x\zeta_y^2 - \varepsilon^2\frac{1}{2}\left(\frac{\partial u'}{\partial z} + \frac{\partial w'}{\partial x}\right)\zeta_x\zeta_y \\ &-\varepsilon\frac{1}{2}\left(\frac{\partial u'}{\partial z} + \frac{\partial v'}{\partial x}\right)\zeta_x(1 + \varepsilon^2\zeta_x^2) - \varepsilon\frac{\partial v'}{\partial y}\zeta_y(1 + \varepsilon^2\zeta_x^2) + \frac{1}{2}\left(\frac{\partial v'}{\partial z} + \frac{\partial w'}{\partial y}\right)\cdot \\ &(1 + \varepsilon^2\zeta_x^2) - \varepsilon^2\frac{1}{2}\left(\frac{\partial u'}{\partial z} + \frac{\partial w'}{\partial x}\right)\zeta_x\zeta_y - \varepsilon^2\frac{1}{2}\left(\frac{\partial v'}{\partial z} + \frac{\partial w'}{\partial y}\right)\zeta_y^2 + \varepsilon\frac{\partial w'}{\partial z}\zeta_y\Big\} \\ = 2\mu'\Big\{&-\varepsilon^3\frac{\partial u}{\partial x}\zeta_x^2\zeta_y - \varepsilon^3\frac{1}{2}\left(\frac{\partial u}{\partial y} + \frac{\partial v}{\partial x}\right)\zeta_x\zeta_y^2 - \varepsilon^2\cdot \\ &\frac{1}{2}\left(\frac{\partial u}{\partial z} + \frac{\partial w}{\partial x}\right)\zeta_x\zeta_y - \varepsilon\frac{1}{2}\left(\frac{\partial u}{\partial y} + \frac{\partial v}{\partial x}\right)\zeta_x(1 + \varepsilon^2\zeta_x^2) - \varepsilon\frac{\partial v}{\partial y}\zeta_y(1 + \varepsilon^2\zeta_x^2) \\ &+\frac{1}{2}\left(\frac{\partial v}{\partial z} + \frac{\partial w}{\partial y}\right)(1 + \varepsilon^2\zeta_x^2) - \varepsilon^2\frac{1}{2}\left(\frac{\partial u}{\partial z} + \frac{\partial w}{\partial x}\right)\zeta_x\zeta_y \\ &-\varepsilon^2\frac{1}{2}\left(\frac{\partial v}{\partial z} + \frac{\partial w}{\partial y}\right)\zeta_y^2 + \varepsilon\frac{\partial w}{\partial z}\zeta_y\Big\} \end{aligned} \tag{A6e}$$

$$u' + w'\varepsilon\zeta_x = u + w\varepsilon\zeta_x \tag{A6f}$$

$$\begin{aligned} &-\varepsilon^2 u'\zeta_x\zeta_y + v'(1 + \varepsilon^2\zeta_x^2) + \varepsilon w'(\zeta_y) \\ &= -\varepsilon^2 u\zeta_x\zeta_y + v(1 + \varepsilon^2\zeta_x^2) + \varepsilon w(\zeta_y). \end{aligned} \tag{A6g}$$

An equivalent set of interfacial conditions at $z = -h(t) + \varepsilon\zeta(x, y, t)$ may also be written with primed quantities replaced by their double-primed equivalents.

Because the interfaces are material surfaces of discontinuity, the kinematic boundary condition (A6a) ensures that the interfaces have the same instantaneous velocity as the adjacent fluid. This interfacial condition is critical to determining the stability of the interface since it determines the evolution of the shape of the interface with time. Equation (A6b) represents the balance of normal velocity across the interface. Equation (A6c) arises from the normal component of momentum balance and represents balance of normal stress across the interface, while (A6d) and (A6e) represent balance of shear stress in

two orthogonal directions tangent to the surface, originating from the tangential component of momentum balance. Finally, (A6f) and (A6g) are adherence conditions that guarantee no relative tangential motion (i.e. welded interfaces) in two orthogonal directions tangent to the interface (for further details, see Alexander 1981, Wollkind & Alexander 1982).

Using the basic velocity distribution given by equation (1) in the text, we consider perturbation solutions to the basic system of equations of the form of equation (4) in the text:

$$\varepsilon\zeta(x, y, t) = 0 + \varepsilon\zeta_1(x, y, t) + O(\varepsilon^2) \tag{A7a}$$

$$u(x, y, z, t) = d_{xx}x + \varepsilon u_1(x, y, z, t) + O(\varepsilon^2) \tag{A7b}$$

$$v(x, y, z, t) = d_{yy}y + s_{yx}x + \varepsilon v_1(x, y, z, t) + O(\varepsilon^2) \tag{A7c}$$

$$w(x, y, z, t) = d_{zz}z + \varepsilon w_1(x, y, z, t) + O(\varepsilon^2) \tag{A7d}$$

$$p(x, y, z, t) = p_0(x, y, z, t) + \varepsilon p_1(x, y, z, t) + O(\varepsilon^2). \tag{A7e}$$

with equivalent expansions for primed and double primed quantities.

Substitution of the solution (A7) into the basic system of equations (A3)–(A5) and the interfacial conditions (A6) and expansion of the interfacial conditions in a Taylor series about $z = h(t)$ yields a series of equations in power of ε. For our analysis, we examine terms of $O(\varepsilon)$ and neglect terms of $O(\varepsilon^2)$. After cancellation of the common factor ε we obtain the following system of linear perturbation equations for $z > h$, $h < z < -h$ and $z < -h$, respectively:

$$\nabla \cdot \mathbf{v}_1' = 0, \qquad -\nabla p_1' + \mu'\nabla^2\mathbf{v}_1' = 0 \tag{A8a–d}$$

$$\nabla \cdot \mathbf{v}_1 = 0, \qquad -\nabla p_1 + \mu\nabla^2\mathbf{v}_1 = 0 \tag{A9a–d}$$

$$\nabla \cdot \mathbf{v}_1'' = 0, \qquad -\nabla p_1'' + \mu''\nabla^2\mathbf{v}_1'' = 0. \tag{A10a–d}$$

For $z = h(t) + \varepsilon\zeta(x, y, t)$:

$$w_1 + e_{zz}\zeta = \frac{\partial\zeta}{\partial t} + xe_{xx}\frac{\partial\zeta}{\partial x} + (ye_{yy} + xs_{yx})\frac{\partial\zeta}{\partial y}, \quad w_1' = w_1 \tag{A11a,b}$$

$$-p_1' + 2r\left(\frac{\partial w_1'}{\partial z}\right) = -p_1 + 2\left(\frac{\partial w_1}{\partial z}\right) \tag{A11c}$$

$$r\left\{-2e_{xx}\zeta_x - s_{yx}\zeta_y + \left(\frac{\partial u_1'}{\partial z} + \frac{\partial w_1'}{\partial x}\right) + 2e_{zz}\zeta_x\right\}$$

$$= \left\{-2e_{xx}\zeta_x - s_{yx}\zeta_y + \left(\frac{\partial u_1}{\partial z} + \frac{\partial w_1}{\partial x}\right) + 2e_{zz}\zeta_x\right\} \tag{A11d}$$

$$r\left\{-s_{yx}\zeta_x - 2e_{yy}\zeta_y + \left(\frac{\partial v_1'}{\partial z} - \frac{\partial w_1'}{\partial y}\right) + 2e_{zz}\zeta_y\right\}$$

$$= 2\left\{-s_{yx}\zeta_x - 2e_{yy}\zeta_y + \left(\frac{\partial v_1}{\partial z} + \frac{\partial w_1}{\partial y}\right) + 2e_{zz}\zeta_y\right\} \tag{A11e}$$

$$u_1' = u_1, \qquad v_1' = v_1. \tag{A11f,g}$$

For $z = -h(t) + \varepsilon\zeta(x, y, t)$ (at the lower interface) an equivalent set of conditions may also be written.

Consistent with the work of Biot (1964), Smith (1975), Fletcher (1977, 1991) and Wollkind & Alexander (1982) we adopt a modified normal mode solution to the system of equations (A8)–(A11). Following Benjamin & Mullin (1988), we consider perturbation solutions given by equations (5) and (6) in the text. [Benjamin & Mullin (1988) considered perturbation velocities of the form:

$$v = \mathbf{V}(k;z)\cos(\alpha x - \beta y),$$

where there is no explicit dependence of the perturbation velocities on the amplitude.] The solutions for the velocities and pressures take the form:

$$[w_1, p_1](x, y, z, t) = [W, P](z;\alpha,\beta)\mathcal{A}(t)\cos(\alpha x - \beta y) \tag{A12a,b}$$

$$[u_1, v_1](x, y, z, t) = [U, V](z;\alpha,\beta)\mathcal{A}(t)\sin(\alpha x - \beta y), \tag{A12c,d}$$

with analogous expansions for primed and unprimed quantities.

To satisfy the two additional boundary conditions of the three-dimensional problem, Fletcher (1991) derived a second independent velocity field, termed the toroidal velocity field, given by:

$$(u_t, v_t, w_t) = (\vartheta(z;\alpha,\beta)(-\alpha\mathcal{A}(t)\sin(\alpha x - \beta y)), -\vartheta(z;\alpha,\beta)(\beta\mathcal{A}(t)\sin(\alpha x - \beta y)), 0). \tag{A13}$$

The total perturbation velocity field is the sum of the two independent velocity fields. Note that:

$$\mathcal{A}(t) = I\exp\left(\int_0^t a(t)\mathrm{d}t\right), \tag{A14}$$

where I is the initial amplitude (Wollkind & Alexander 1982). In what follows, I is treated as an arbitrary constant.

To solve for the z-dependent parts of equations (A12) and (A13), these equations are substituted into the Navier–Stokes equations (A8)–(A11) and solved for W and ϑ, giving:

$$(D^2 - \omega^2)^2 W = 0 \tag{A15}$$

and

$$(D^2 - \omega^2)\vartheta = 0. \tag{A16}$$

Equation (A15) has the solution (Fletcher 1977, 1991, Alexander 1981):

$$W(z;\omega) = [A + B(\omega z - 1)]e^{\omega z} - [C + D(\omega z + 1)]e^{-\omega z}. \tag{A17}$$

Equation (A16) is a second-order equation that has the general solution (Fletcher 1991):

$$\vartheta(z;\omega) = Fe^{\omega z} + Ge^{-\omega z}. \tag{A18}$$

From equations (A8)–(A10), (A17) and (A18), the perturbation velocity and pressure components may be derived:

$$w_1 = \{[A + B(\omega z - 1)]e^{\omega z} - [C + D(\omega z + 1)]e^{-\omega z}\}$$
$$\mathcal{A}(t)\cos(\alpha x - \beta y) \tag{A19a}$$

$$p_1 = 2\omega(Be^{\omega z} - De^{-\omega z})\mathcal{A}(t)\cos(\alpha x - \beta y) \tag{A19b}$$

$$u_1 = (-\alpha/\omega\{[A + B\omega z]e^{\omega z} + [C + D\omega z]e^{-\omega z}\}$$
$$-\beta/\omega^2\{Fe^{\omega z} + Ge^{-\omega z}\})\mathcal{A}(t)\sin(\alpha x - \beta y) \tag{A19c}$$

$$v_1 = (\beta/\omega\{[A + B\omega z]e^{\omega z} + [C + D\omega z]e^{-\omega z}\}$$
$$-\alpha/\omega^2\{Fe^{\omega z} + Ge^{-\omega z}\})\mathcal{A}(t)\sin(\alpha x - \beta y), \tag{A19d}$$

with equivalent expressions for the primed and double-primed quantities.

The total flow (u, v, w) must reduce to the basic flow (u_0, v_0, w_0) far from the layer (see Ramberg 1962).

$$\mathbf{v}_1' \to 0, \qquad p_1' \to 0 \qquad \text{as } z \to +\infty \tag{A20a}$$

and

$$\mathbf{v}_1'' \to 0, \qquad p_1'' \to 0 \qquad \text{as } z \to -\infty. \tag{A20b}$$

Satisfaction of these conditions (Fletcher 1991) requires that:

$$A' = B' = F' = C'' = D'' = G'' = 0. \tag{A21}$$

Furthermore, imposing the symmetry requirements discussed by Treagus (1973), Smith (1975) and Fletcher (1977, 1991), a fold-like disturbance requires that w_1 is even in z:

$$W(z;\omega) = W(-z;\omega) \tag{A22a}$$

and

$$W'(z;\omega) = W''(-z;\omega), \tag{A22b}$$

so

$$A = -C;\ B = D;\ F = G;\ A'' = -C';\ B'' = D';$$
and
$$F'' = G'. \tag{A23a–f}$$

The velocities and pressures in the layer are then:

$$w_1 = \{[A + B(\omega z - 1)]e^{\omega z} - [(-A) + B(\omega z + 1)]e^{-\omega z}\}$$
$$\mathcal{A}(t)\cos(\alpha x - \beta y) \tag{A24a}$$

$$p_1 = 2\omega(Be^{\omega z} - Be^{-\omega z})\mathcal{A}(t)\cos(\alpha x - \beta y) \tag{A24b}$$

$$u_1 = (-\alpha/\omega\{[A + B\omega z]e^{\omega z} + [(-A) + B\omega z]e^{-\omega z}\}$$
$$-\beta/\omega^2\{Fe^{\omega z} + Fe^{-\omega z}\})\mathcal{A}(t)\sin(\alpha x - \beta y) \tag{A24c}$$

$$v_1 = (-\beta/\omega\{[A + B\omega z]e^{\omega z} + [(-A) + B\omega z]e^{-\omega z}\}$$
$$-\alpha/\omega^2\{Fe^{\omega z} + Fe^{-\omega z}\})\mathcal{A}(t)\sin(\alpha x - \beta y), \tag{A24d}$$

while those in the upper and lower media are:

$$w_1' = w_1'' = \{-[C' + D'(\omega z + 1)]e^{-\omega z}\}\mathcal{A}(t)\cos(\alpha x - \beta y) \quad \text{(A25a)}$$

$$p_1' = p_1'' = -2\omega D' e^{-\omega z}\mathcal{A}(t)\cos(\alpha x - \beta y) \quad \text{(A25b)}$$

$$u_1' = u_1'' = \{-\alpha/\omega[C' + D'\omega z]e^{-\omega z} - \beta/\omega^2 G' e^{-\omega z}\}\mathcal{A}(t)\sin(\alpha x - \beta y) \quad \text{(A25c)}$$

$$v_1' = v_1'' = \{\beta/\omega[C' + D'\omega z]e^{-\omega z} - \alpha/\omega^2 G' e^{-\omega z}\}\mathcal{A}(t)\sin(\alpha x - \beta y). \quad \text{(A25d)}$$

Substitution of (A24) and (A25) into the interfacial conditions (A11) yields the following systems of equations (not writing out $U(z)$, $V(z)$, $P(z)$ and $W(z)$ in full):

$$\frac{d\mathcal{A}}{dt} = \mathcal{A}(t)(e_{zz} + W(z)), \qquad W'(z) = W(z) \quad \text{(A26a,b)}$$

$$P'(z) - 2r(DW'(z)) = P(z) - 2(DW(z)) \quad \text{(A26c)}$$

$$r(\beta + DU'(z) - \alpha W'(z)) = \beta + DU(z) - \alpha W(z) \quad \text{(A26d)}$$

$$r(-\alpha + DV'(z) + \beta W'(z)) = -\alpha + DV(z) + \beta W(z) \quad \text{(A26e)}$$

$$U'(z) = U(z), \qquad V'(z) = V(z), \quad \text{(A26f,g)}$$

where $D = d/dz$.

There are seven unknown constants A, B, C', D', F, G' and I, and seven interfacial conditions at each interface with which to evaluate them. Due to the imposed symmetries the system at $z = h$ is identical to the system at $z = -h$ and it is sufficient to examine the behavior of only one interface to determine the stability of the layer as a whole (Smith 1975, Fletcher 1977, 1991, Wollkind & Alexander 1982). To evaluate the unknown constants the system of equations (A26), representing a system of linear homogeneous equations in the quantities A, B, C', D', F, G', is solved yielding the secular equation given by equation (7) in the main text.

Pinch-and-swell mode

For a symmetric pinch-and-swell deformation the z-component of w_1 is odd (Smith 1975) and we have:

$$-W(z;\omega) = W(-z;\omega) \quad \text{(A27a)}$$

and

$$-W'(z;\omega) = W''(-z;\omega), \quad \text{(A27b)}$$

which gives the relation for the constants in equation (A20):

$$C = A;\ D = -B;\ G = -F;\ A'' = C';\ B'' = -D';\ \text{and}\ F'' = -G'. \quad \text{(A28a–f)}$$

The perturbation velocities in the layer are then:

$$w_1 = \{[A + B(\omega z - 1)]e^{\omega z} - [A - B(\omega z + 1)]e^{-\omega z}\}\mathcal{A}(t)\cos(\alpha x - \beta y) \quad \text{(A29a)}$$

$$p_1 = 2\omega(Be^{\omega z} + Be^{-\omega z})\mathcal{A}(t)\cos(\alpha x - \beta y) \quad \text{(A29b)}$$

$$u_1 = (-\alpha/\omega\{[A + B\omega z]e^{\omega z} + [A - B\omega z]e^{-\omega z}\} - \beta/\omega\{Fe^{\omega z} - Fe^{-\omega z}\})\mathcal{A}(t)\sin(\alpha x - \beta y) \quad \text{(A29c)}$$

$$v_1 = (\beta/\omega\{[A + B\omega z]e^{\omega z} + [A - B\omega z]e^{-\omega z}\} - \alpha/\omega^2\{Fe^{\omega z} - Fe^{-\omega z}\})\mathcal{A}(t)\sin(\alpha x - \beta y), \quad \text{(A29d)}$$

while those in the upper and lower media are

$$w_1' = w_1'' = \{-[C' - D'(\omega z + 1)]e^{-\omega z}\}\mathcal{A}(t)\cos(\alpha x - \beta y) \quad \text{(A30a)}$$

$$p_1' = p_1'' = -2\omega D' e^{-\omega z}\mathcal{A}(t)\cos(\alpha x - \beta y) \quad \text{(A30b)}$$

$$u_1' = u_1'' = (-\alpha/\omega[C' + D'\omega z]e^{-\omega z} - \beta/\omega^2 G' e^{-\omega z})\mathcal{A}(t)\sin(\alpha x - \beta y) \quad \text{(A30c)}$$

$$v_1' = v_1'' = (\beta/\omega[C' + D'\omega z]e^{-\omega z} - \alpha/\omega^2 G' e^{-\omega z})\mathcal{A}(t)\sin(\alpha x - \beta y). \quad \text{(A30d)}$$

Proceeding in a fashion similar to the folding problem, substitution of equations (A29) and (A30) into the interfacial conditions yields a system of equations which may be solved to give the secular equation (10) in the main text.